

Excellent Specific Mechanical and Electrical Properties of Anisotropic Freeze-Cast Native and Carbonized Bacterial Cellulose-Alginate Foams

Kaiyan Qiu and Ulrike G. K. Wegst*

Native and carbonized freeze-cast bacterial cellulose-alginate (BC-ALG) foams possess an ice-templated honeycomb-like architecture with remarkable properties. Their unique pore morphology consists of two levels of porosity: 20–50 μm diameter pores between, and 0.01–10 μm diameter pores within the cell-walls. The mechanical properties of the BC-ALG foams, a Young's modulus of up to 646.2 ± 90.4 kPa and a compressive yield strength of up to 37.1 ± 7.9 kPa, are high for their density and scale as predicted by the Gibson–Ashby model for cellular materials. Carbonizing the BC-ALG foams in an inert atmosphere at 1000–1200 $^{\circ}\text{C}$ in a second processing step, both pore morphology and mechanical properties of the BC-ALG remain well preserved with specific mechanical properties that are higher than those reported in the literature for similar foams. Also the electrical conductivity of the BC-ALG foams is high at 1.68 ± 0.04 S cm^{-1} at a density of only 0.055 g cm^{-3} , and is found to increase with density as predicted, and as a function of the degree of carbonization determined by both carbonization temperature and atmosphere. The property profile makes freeze-cast BC-ALG foams and their carbonized foams attractive for energy applications and as a sorbent.

1. Introduction

Bacterial cellulose (BC), produced by certain bacteria (usually *Gluconacetobacter*) in a fermentation process, is a sustainable nanofibrous biomaterial that has the same polysaccharide structure as plant-based cellulose.^[1–7] BC is composed of nanofibers with diameters in the range of 40–70 nm and has many unique characteristics including high purity, a high degree of

polymerization, high crystallinity (typically up to 70%), which results in an estimated Young's modulus of 114 GPa for a single BC nanofiber.^[8] BC also possesses a high water-holding capacity, high thermal stability up to 260 $^{\circ}\text{C}$, good biocompatibility and excellent biodegradability.^[1,9–12] Both the thickness and weight of the pellicles that the bacteria grow can be controlled and depend on culture media type and concentration, bacteria seed liquid amount, and culture time.^[1,2,4,5] The BC pellicle shape can be controlled by culture vessel shape, shaking speeds, etc. Because of their attractive material properties, BC-based materials are explored, in research and commercially, for a broad range of applications including foods (nata-de-coco),^[1,13] high quality paper,^[1] cosmetics and textiles,^[4] artificial skin and blood vessels,^[14,15] artificial bone and scaffold,^[16] antimicrobial substrates,^[1] as binding agent for fibers and other materials,^[17]

loud-speaker diaphragms,^[1] and functional nanocomposites for high-strength materials,^[2–4,7,18] as well as materials in optical and luminescent,^[1,13] catalytic and proton conductive,^[1] thermo-responsive,^[1] and separating^[19] applications. However, at the time of the writing of this article, complex culture processes still pose obstacles to low-cost production at industrial scale and costs remain comparatively high for BC-based materials.

A processing technique that ideally lends itself for the manufacture of BC-based foams, here using alginate (ALG) as a binder, for either direct application or further processing by carbonization, is freeze casting, the directional solidification of aqueous solutions or slurries, with which complex and well-controlled pore structures can be achieved. Freeze casting is a two-step process: first an aqueous solution or slurry is directionally solidified, causing a phase separation to occur, because water freezes pure. In the second processing step, the ice phase is removed from the freeze-cast sample by sublimation.^[20–29] The result is a scaffold or foams, whose microstructure is templated by the ice crystals during freezing.^[20–29] Because the freezing conditions and through it the materials structure and properties can be carefully controlled, freeze casting offers an attractive and straightforward approach to the manufacture of hierarchically structured materials and foams for a variety of applications, particularly those that benefit from the two levels of porosity of the scaffolds: microscopic pores of 20–50 μm

K. Qiu, U. G. K. Wegst
Thayer School of Engineering
Dartmouth College
Hanover, NH 03755, USA
E-mail: u.wegst@northeastern.edu

K. Qiu
School of Mechanical and Materials Engineering
Washington State University
Pullman, WA 99164, USA
U. G. K. Wegst
Department of Physics
Northeastern University
Boston, MA 02115, USA

 The ORCID identification number(s) for the author(s) of this article can be found under <https://doi.org/10.1002/adfm.202105635>.

DOI: 10.1002/adfm.202105635

diameter forming a honeycomb-like structure and 0.01–10 μm diameter pores within the cell walls.^[20]

Carbonaceous foams have attracted a considerable research interest in recent years, because they combine exceptionally low densities and a high specific surface area with considerable stiffness and strength, and high electrical conductivity.^[30–39] Applications for which they are thought to be particularly promising include electrodes and supercapacitors, sensors and actuators, and other electronic devices that benefit from high specific electrical properties.^[30–39] One approach to manufacture carbonaceous foams is to first freeze cast BC foams and then to carbonize them.

Reported in this contribution are the manufacture and properties of foams made by freeze casting, their structural characterization by scanning electron microscopy (SEM) before and after carbonization, the quantification of the degree of carbonization of the carbonized BC-ALG by Raman spectroscopy, their mechanical testing in compression, and the determination of their electrical properties using a four-point probe. Particularly, the mechanical and electrical properties were found to exceed those reported in the literature for BC-based materials of comparable density.

2. Results and Discussion

2.1. The Microstructure of Freeze-Cast BC-ALG Foams and Carbonized Freeze-Cast BC-ALG Foams

2.1.1. The Structure of BC Pellicles, Cryomilled BC Particles, Freeze-Cast BC-ALG Foams and Carbonized Freeze-Cast BC-ALG Foams

A typical BC pellicle produced by *Gluconacetobacter* in static fermentation is shown in **Figure 1A**. After cryomilling, the BC pellicle is broken into micrometer-scale BC particles with a typical diameter of 20–100 μm , such as the one shown in **Figure 1B**. The SEM micrograph of **Figure 1C**, which is a magnification of the area marked by the red square, shows that these BC particles retain a nanometer-scale pore structure after cryomilling. The mean diameter of the BC-nanofibers in the cryomilled pellicle particles was less than 100 nm and the pore diameters ranged from several tens to several hundred nanometers. The cryomilled BC particles were used for the manufacture of the freeze-cast BC-ALG composite described in this study. Typical freeze-cast BC-ALG foams before (left) and after (right) carbonization are shown in **Figure 1D**. The density of freeze-cast BC-ALG foams is typically

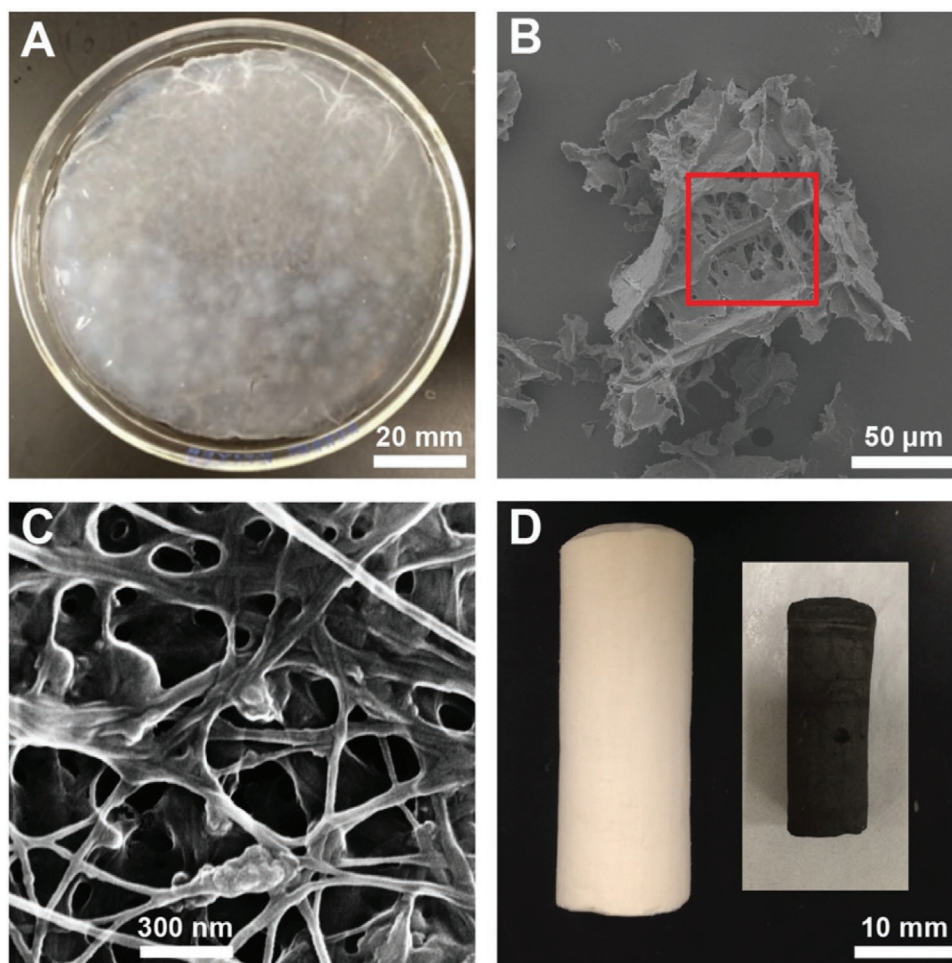


Figure 1. BC formation, freeze-cast BC-ALG foam, and carbonized freeze-cast BC-ALG foam. A) BC pellicle. B) SEM micrograph of freeze-dried BC particles obtained after cryomilling. C) SEM micrograph of nanometer-scale pore structure of the freeze-dried BC particles after cryomilling, a magnification of the area marked by the red square in (B). D) Freeze-cast BC-ALG foam (left) and carbonized freeze-cast BC-ALG foam (right).

$0.055 \pm 0.002 \text{ g cm}^{-3}$ (middle layer). After carbonization, the foam density of the middle layer decreases to $0.042\text{--}0.044 \text{ g cm}^{-3}$ (1000 and 1100 °C) and $0.052 \pm 0.003 \text{ g cm}^{-3}$ (1200 °C), because of the removal of side groups, elements other than carbon, and likely a small, unavoidable amount of oxidation. In addition to a considerable weight loss, carbonization also leads to a considerable (40%) shrinkage in both diameter and height, to about 60% of their original values. However, the shrinkage is not proportional to increasing carbonization temperature, as indicated by the observed density changes.

Reported in the literature is that, even after up to 85% volume shrinkage, the density of freeze-dried BC decreases significantly when carbonized,^[30,34,37] and that, in fact, the weight loss effect dominates the size shrinkage effect and leads to considerably lower densities, particularly, when carbonization occurs at high temperatures (in the range of 600–1450 °C).^[30,34,37,40] However, in our case, the density values for foams carbonized at 1200 °C remained similar to that before carbonization, which suggests that shrinkage and weight loss occur to a comparable extent.

2.1.2. Porous Structure of Freeze-Cast BC-ALG Foams Before and After Carbonization

The SEM micrographs of Figures 2A–D show cross sections of a BC-ALG foam, before (A,B) and after (C,D) carbonization, cut perpendicular (A,C) and parallel (B,D) to the freezing direction. Figure 2A illustrates the geometry and size distribution of the micrometer-scale porosity; on average their lengths and widths

are 24.1 ± 9.3 and $13.3 \pm 3.1 \mu\text{m}$, respectively, resulting in a pore aspect ratio of 1.8 ± 0.4 . The high standard deviations indicate the large range in size and shape. Figure 2B reveals the web-like structure of the cell wall material in the freeze-cast BC-ALG foams, by which the highly aligned pores are connected in the scaffold. The SEM micrograph further reveals how ALG binds and tightly connects the BC particles with each other. In addition to the ice-templated micrometer-scale porosity of the scaffolds, the BC-ALG cell wall material exhibits a pore size distribution from the nanometer to the micrometer scale, which we hypothesize, likely results from the original nanoporosity of the BC-pellicles and the porosity that forms when the fibers assemble into a fiber mat during freeze casting. As a result, freeze-cast BC-ALG foams possess a unique architecture. Figure 2C shows that the pore morphology of freeze-cast BC-ALG foam was maintained after carbonization, that the average pore lengths and widths decreased by about 33% to 16.0 ± 5.0 and $8.4 \pm 2.8 \mu\text{m}$, respectively, but that with a value of 1.9 ± 0.3 the pore aspect ratio remained almost the same. These linear shrinkage values explain the 40% shrinkage in diameter and length of the carbonized cell walls, respectively, so that after carbonization the freeze-cast BC-ALG foam possesses about 20–25% of its original volume.

2.2. Electrical Conductivity for Carbonized Freeze-Cast BC-ALG Foams

A comparison of the densities and electrical conductivities of freeze-cast BC-ALG foams carbonized at different temperatures

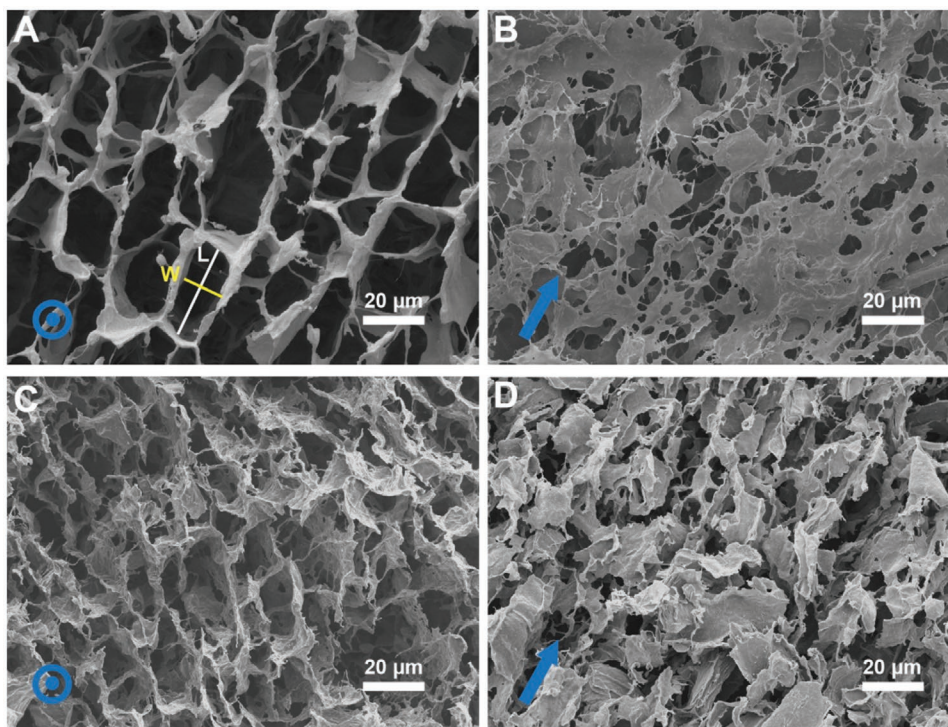


Figure 2. Structures of freeze-cast BC-ALG foam and carbonized freeze-cast BC-ALG foam. A,B) SEM micrographs of cross sections cut perpendicular (A) and parallel (B) to the freezing direction in freeze-cast BC-ALG foam (W: width, L: length in Figure 2A for pore size measurement demonstration). C,D) SEM micrographs of cross sections cut perpendicular (C) and parallel (D) to the freezing direction in carbonized freeze-cast BC-ALG foam. The blue circles indicate the cross sections parallel to the freezing direction and the blue arrows indicate the freezing direction.

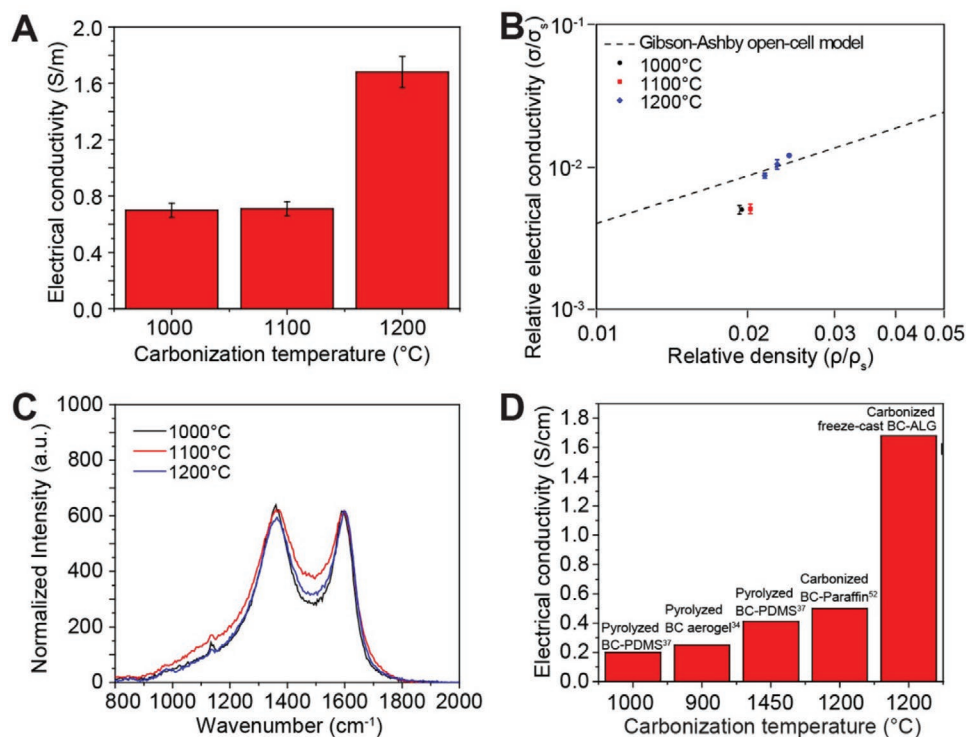


Figure 3. Electrical properties of carbonized freeze-cast BC-ALG foam. A) Correlation between electrical conductivity and carbonization temperatures for the carbonized freeze-cast BC-ALG foams; B) correlation between electrical conductivity and relative density for the carbonized freeze-cast BC-ALG foams processed at 1000 °C ($\rho = 0.044 \text{ g cm}^{-3}$), 1100 °C ($\rho = 0.046 \text{ g cm}^{-3}$), 1200 °C ($\rho = 0.049 \text{ g cm}^{-3}$ (top); $\rho = 0.052 \text{ g cm}^{-3}$ (middle); $\rho = 0.055 \text{ g cm}^{-3}$ (bottom)) and a comparison with the Gibson–Ashby open cell model;^[41–43] C) Raman spectra of the carbonized freeze-cast BC-ALG foams processed at different carbonization temperatures; D) Electrical conductivity comparison for carbonized freeze-cast BC-ALG foam and other carbonized BC-based aerogels/foams.

reveals both an increase in density and degree of carbonization, and as a result, a significant increase in electrical conductivity. Samples carbonized at 1200 °C had with $1.68 \pm 0.04 \text{ S cm}^{-1}$ more than twice the electrical conductivity of samples carbonized at 1000 °C ($0.70 \pm 0.02 \text{ S cm}^{-1}$) and 1100 °C ($0.71 \pm 0.02 \text{ S cm}^{-1}$), shown in **Figure 3A**. Exploring, whether carbonization at still higher temperatures would result in even higher electrical conductivities, we found that samples carbonized at temperatures above 1200 °C not only lost their mechanical integrity, but also had a lower electrical conductivity.

The main reasons for the high electrical conductivity observed in the foams processed at 1200 °C is its density of $0.052 \pm 0.003 \text{ g cm}^{-3}$ (middle layer), which is higher than that of foams carbonized at 1000 and 1100 °C, whose mean densities fall within the range of $0.044\text{--}0.046 \text{ g cm}^{-3}$. The freeze-cast BC-ALG foam carbonized at 1200 °C shrank more than others, resulting in a higher density. Additionally, the densities of top, middle, and bottom layers of samples carbonized at 1200 °C were found to differ with values of 0.049, 0.052, and 0.055 g cm^{-3} , respectively. This is because the shrinkage for top, middle, and bottom layers differ as shown in **Figure 1D** where the top part of the carbonized BC-ALG foam remains considerably larger in volume than the bottom part.

Figure 3B shows that the relative electrical conductivity increases with increasing relative density in freeze-cast BC-ALG foams carbonized at 1000, 1100, and 1200 °C as predicted by the

open cell foam model of Gibson and Ashby, assuming a similar degree of carbonization in all samples.^[41–43]

$$\frac{\sigma}{\sigma_s} = \frac{1}{3} \frac{\rho}{\rho_s} + 2 \left(\frac{\rho}{\rho_s} \right)^{\frac{3}{2}} \quad (1)$$

where σ is the electrical conductivity and ρ the density of the scaffold, σ_s is the electrical conductivity, and ρ_s the density of the solid, from which the scaffold is formed. Assuming an electrical conductivity of $\sigma_s = 140 \text{ S cm}^{-1}$ and a density of $\rho_s = 2.25 \text{ g cm}^{-3}$ for the scaffold solid,^[44–49] the mean values obtained for solid carbon films carbonized at 1200 °C perfectly fit the model as shown in **Figure 3B**. The fit of the value of $\sigma_s = 140 \text{ S cm}^{-1}$ indicates that the degree of carbonization results in the presence of both amorphous carbon and graphitic carbon, but that amorphous carbon dominates.^[44,50,51] In contrast, the average data points from the samples carbonized at 1000 and 1100 °C fall below the prediction.

The results suggest that a combination of higher material density and degree of carbonization result in the higher electrical conductivity of freeze-cast BC-ALG foams carbonized at higher temperatures. The Raman spectra for aerogels carbonized in the range of 1000–1200 °C shown in **Figure 3C** supports this. The spectra show the two peaks associated with sp^2 (D- and G-band) hybridizations of carbon, where the D

and G bands correspond to disordered or polycrystalline and ordered or crystalline graphite, respectively; the intensity of the D peak at 1330 cm^{-1} decreases and that of the G peak at 1590 cm^{-1} increases with increasing carbonization temperature. As a result, also the ratio of the intensities of the D band to the G band $R = I_D/I_G$ decreases with increasing carbonization temperature, with a lower R value indicating both an increase in the degree of carbonization (graphitization) and structural order.^[33] While the decrease in R value is small for freeze-cast BC-ALG foams, when the carbonization temperature increases from 1000 to $1100\text{ }^\circ\text{C}$, it is significant for a further increase in carbonization temperature to $1200\text{ }^\circ\text{C}$. Thus, the electrical conductivity of the carbonized freeze-cast BC-ALG foams can be tailored to an application by controlling their densities and degree of carbonization through the choice of material composition, carbonization condition, and temperature.

The electrical conductivity of the carbonized freeze-cast BC-ALG foam in the study was higher than that reported for carbonized BC-based foams in the literature. Typical literature values range from 0.20 – 0.41 S cm^{-1} with 0.25 S cm^{-1} for pyrolyzed BC ($\rho = 0.01\text{ g cm}^{-3}$).^[34,37,52] Figure 3D shows a comparison of the electrical conductivity of our experimental values for freeze-cast BC-ALG foams carbonized at $1200\text{ }^\circ\text{C}$ with literature values for BC-based foams carbonized at temperatures in the range of 900 – $1450\text{ }^\circ\text{C}$. Since the density of the latter materials is frequently not provided, we have to speculate. However, the freeze-cast BC-ALG foams outperform those described in the literature probably due to a higher density, different pore structure, and morphology, and a higher degree of carbonization achieved at $1200\text{ }^\circ\text{C}$. A comparison with carbonized plant-based nanocellulose or regenerated cellulose is difficult, because there is no literature on carbonized samples prepared purely from these, but only on composites with more conductive additives such as graphene oxide^[53] or carbon nanotubes.^[54] As a result, a fair comparison of their electrical conductivity with our carbonized BC-ALG foams is not possible.

2.3. Mechanical Properties of Freeze-Cast BC-ALG Foams and Carbonized Freeze-Cast BC-ALG Foams

Compression tests were performed on the freeze-cast BC-ALG foams before and after carbonization, because compression is the dominating loading condition in most applications for which foams have shown promise.^[27,28] Figure 4A shows typical cubic test samples with a side-length of 5 mm of the freeze-cast BC-ALG foam (left) and carbonized freeze-cast BC-ALG foam (right). The cubes were tested parallel and perpendicular to the freezing direction. To remove initial slack, the origin of the stress–strain curve was defined as the intersection between the tangent line of the initial elastic region. Young's modulus, yield strength and toughness were determined from the corrected stress–strain curves, for which a typical example is shown in Figure 4B. Young's modulus was determined from the slope of the initial elastic linear region, while the yield strength was determined from the point of intersection between the tangent line to the elastic region and the tangent line of the plateau or collapse region. Toughness was determined from the area under the stress–strain curve from 0% to 60% strain.^[27,28]

Figures 4C,D show typical stress–strain curves of the freeze-cast BC-ALG samples before and after carbonization for the three layers within the sample (top, middle, and bottom), tested parallel and perpendicular to the freezing direction, respectively. Figures 4C,D reveal that the bottom layers of the freeze-cast BC-ALG and the carbonized freeze-cast BC-ALG test samples have higher mechanical properties than the corresponding middle and top layers; this is because the density decreases from the bottom to the top layer. Figures 4C,D also show that the mechanical properties of the samples tested parallel to the freezing direction are typically 1.5 – 2.5 times higher than the same samples tested perpendicular to the freezing direction.

A detailed comparison of mechanical properties of freeze-cast BC-ALG foams and carbonized freeze-cast BC-ALG foams is shown in Table 1. The data of Young's modulus and yield strength can be expected to scale with the relative density according to the Gibson–Ashby model. Equations (2)–(5) state the correlations for honeycombs (stretch-dominated behavior) and foams (bending-dominated behavior), where E_h , E_f , and E_s are the Young's moduli, σ_h , σ_f , and σ_s are the yield strengths, and ρ_h , ρ_f , and ρ_s are the densities, of the honeycomb, the foam, and, respectively, and C_1 , C_2 , C_3 , C_4 are constants^[28,41,55–57]

$$E_h = C_1 E_s (\rho_h / \rho_s) \quad (2)$$

$$\sigma_h = C_2 \sigma_s (\rho_h / \rho_s) \quad (3)$$

$$E_f = C_3 E_s (\rho_f / \rho_s)^2 \quad (4)$$

$$\sigma_f = C_4 \sigma_s (\rho_f / \rho_s)^{3/2} \quad (5)$$

The freeze-cast BC-ALG and carbonized BC-ALG foams of this study possess similar honeycomb-like structures and the corresponding compositions are known. Literature values for dried solid BC sheet properties have a wide range; we chose as typical material property values $\rho_s = 1.50\text{ g cm}^{-3}$, $E_s = 320\text{ MPa}$, and $\sigma_s = 16730\text{ kPa}$.^[2,3,58,59] Similarly, we chose for solid carbon, the typical values of $\rho_s = 2.25\text{ g cm}^{-3}$, $E_s = 2.3\text{ GPa}$, and $\sigma_s = 31\text{ MPa}$.^[60] Using these, the experimental results of Table 1 were compared to the Gibson–Ashby model and predictions.^[3] Figures 4E,F show how the experimental data points for modulus (E) and strength (F) compare with the Gibson–Ashby model and correlation of relative Young's modulus and relative density for both freeze-cast BC-ALG and carbonized BC-ALG foams, tested both parallel and perpendicular to the freezing direction.

Overall, the observed mechanical performance reflects the anisotropic structure of the material. Higher values are observed parallel to the freezing direction, due to the preferential structural alignment in the foam caused during the freezing process; lower values are observed perpendicular to the freezing direction, which has a structure more akin to a foam than a honeycomb. All values fall underneath the honeycomb and foam model lines, respectively, when assuming $C = 1$. The experimental values are lower than those for an ideal honeycomb structure, because the structures of both BC-ALG and carbonized BC-ALG foams are not perfect honeycombs or foam, but are slightly wavy and as a result misaligned with the loading direction; additionally, they have variations in their

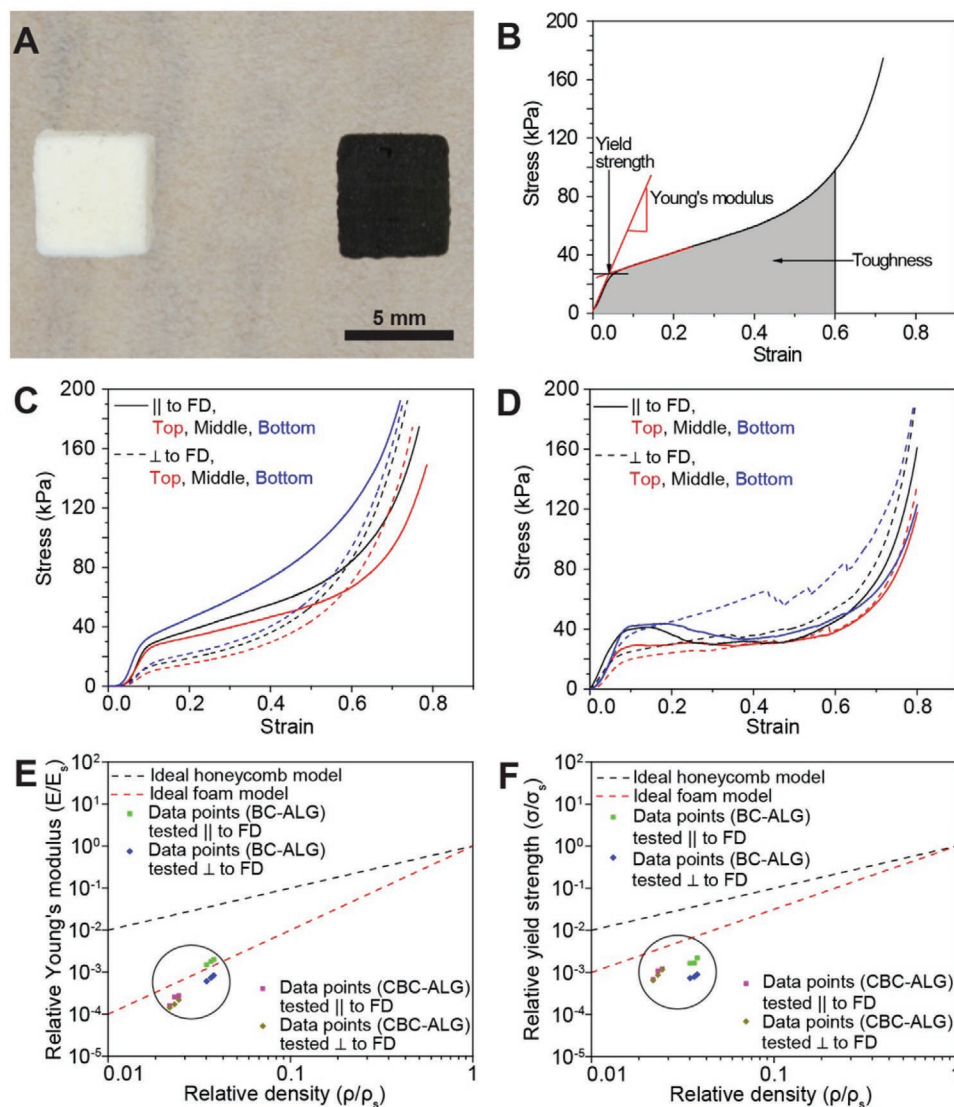


Figure 4. Mechanical properties of freeze-cast BC-ALG foam and carbonized freeze-cast BC-ALG foam. A) Typical cubes prepared from freeze-cast BC-ALG foam (left) and carbonized freeze-cast BC-ALG foam (right) for mechanical testing. B) Typical stress–strain curve of a sample for determining Young’s modulus, yield strength and toughness. C) Typical stress–strain curves of freeze-cast BC-ALG cubic samples at top, middle, and bottom layers tested parallel and perpendicular to the freezing direction (FD). D) Typical stress–strain curves of carbonized freeze-cast BC-ALG cubic samples at top, middle and bottom layers tested parallel and perpendicular to the freezing direction (FD). E) Correlation of relative Young’s modulus and relative density for both freeze-cast BC-ALG and carbonized BC-ALG (CBC-ALG) foams and the corresponding Gibson–Ashby models for honeycombs and foams. F) Correlation of relative yield strength and relative density for both freeze-cast BC-ALG and carbonized BC-ALG (CBC-ALG) foams and the corresponding Gibson–Ashby models for honeycomb and foam.

local microstructure, both leading to lower mechanical properties.^[41] Finally, our comparison with literature values neglects the differences that results from the specific cell wall material structure and properties E_s and σ_s that are unique for each foam composition and processing condition.^[27,28]

Carbonized freeze-cast BC-ALG foams show excellent compressive mechanical properties in addition to their high electrical conductivity. The bottom layer has an average Young’s modulus and yield strength of up to 633.1 and 377 kPa (0.055 g cm^{-3}), respectively, thus values that are higher than those previously reported for carbonized BC foams. Stated in the literature are a compressive strength of 2.5 kPa at 80%

strain ($0.003\text{--}0.004 \text{ g cm}^{-3}$)^[37] and less than 10 kPa compressive strength at 80% strain ($0.004\text{--}0.006 \text{ g cm}^{-3}$).^[30] The values are also higher than a recent report for carbonized BC-Poly(amic acid) foam, for which, unfortunately, no modulus and density values were provided, making a true comparison impossible,^[61] since both density as well as the unique anisotropic structure for carbonized freeze-cast BC-ALG foams contribute to their higher mechanical properties. The comparatively higher mechanical properties for the carbonized freeze-cast BC-ALG foam of this study broaden their range of applications to include their use as supercapacitors,^[61,63,64] electrodes for batteries,^[34] conductors for LEDs,^[37] or absorbents for the removal of organic solvents.^[30,61,62]

Table 1. Comparison of mechanical properties of native freeze-cast BC-ALG foams and carbonized freeze-cast BC-ALG foams.

Composition	Direction of testing with respect to freezing direction	Density [g cm ⁻³]	Young's Modulus [kPa]	Yield Strength [kPa]	Toughness [kJ m ⁻³]
Native freeze-cast BC-ALG foams					
Top layer		0.052	475.9 ± 48.3	27.3 ± 0.9	24.2 ± 2.1
	⊥		196.0 ± 23.9	12.3 ± 0.2	18.6 ± 0.1
Middle layer		0.055	574.3 ± 49.5	27.8 ± 0.4	30.7 ± 0.8
	⊥		234.6 ± 9.9	13.2 ± 1.2	22.8 ± 0.5
Bottom layer		0.057	646.2 ± 90.4	37.1 ± 7.9	42.2 ± 1.9
	⊥		268.0 ± 27.9	15.0 ± 0.8	25.2 ± 0.4
Carbonized freeze-cast BC-ALG foams					
Top layer		0.049	372.6 ± 26.1	21.2 ± 0.7	17.0 ± 1.4
	⊥		332.3 ± 41.8	20.1 ± 1.7	12.3 ± 4.1
Middle layer		0.052g	594.7 ± 2.8	33.9 ± 5.9	19.8 ± 1.4
	⊥		394.5 ± 10.1	27.1 ± 3.7	16.7 ± 2.9
Bottom layer		0.055g	633.1 ± 44.8	37.7 ± 2.8	26.0 ± 5.1
	⊥		506.5 ± 12.6	36.5 ± 2.2	29.6 ± 3.5

Listed in Table 1 are Young's modulus and yield strength obtained in tests parallel to the freezing direction for the different BC-ALG foams. Interestingly, these values did not change significantly due to the carbonization, while both the Young's modulus and yield strength perpendicular to the freezing direction increased significantly for the carbonized freeze-cast BC-ALG foams, even though the carbonized BC-ALG foams have densities very similar to their corresponding freeze-cast BC-ALG foams.

3. Conclusions

BC-ALG foams were manufactured by freeze casting and their structural, mechanical, and electrical properties tested and compared before and after carbonization at temperatures from 1000 to 1200 °C. Both foams possess unique architectures with porosities at the micrometer and nanometer scales, low densities, and high specific mechanical properties. When carbonized, the freeze-cast BC-ALG foams additionally possess a high electrical conductivity, while maintaining their hierarchical pore structure, low density, and high specific mechanical properties. When it comes to applications, the freeze-cast BC-ALG foams are suitable as scaffolds for tissue regeneration with a structure, shape, and properties that can be tailored for a specific application. When carbonized, BC-ALG foams additionally have attractive electrical conductivities that can be tailored for a given application through composition and processing conditions to obtain the desired degree of carbonization. The mechanical and electrical properties of the two foam types match those predicted by the Gibson–Ashby models. The structural, mechanical, and electrical properties observed in our native and carbonized BC-ALG foams are superior to those reported in the

literature for similar density. Based on the successful application of materials with a similar property profile as absorbents for the removal of organic solvents,^[30,61,62] and as electrodes and supercapacitors,^[34,61,63,64] further exploration of BC-ALG-based foams for these applications appears to be of merit.

4. Experimental Section

Materials: D-Mannitol (white to off-white powder), tryptone (product of New Zealand), yeast extract (molecular genetics powder), and agar (product of Morocco) were obtained from Fisher Scientific (Waltham, MA). Sodium alginate (from brown algae) was purchased from Sigma-Aldrich (St. Louis, MO) with a mannuronic acid/guluronic acid ratio of 0.92.^[65,66] All chemicals were used as received and without further purification. *Gluconacetobacter hansenii* (ATCC 23769) was obtained from the American Type Culture Collection (ATCC, Manassas, VA) for bacterial cellulose culture.

Preparation of BC Pellicles: *Gluconacetobacter hansenii*, ATCC 23769, was used as the model strain and maintained on agar plates containing 25 g L⁻¹ D-mannitol, 5 g L⁻¹ yeast extract, 5 g L⁻¹ tryptone, and 20 g L⁻¹ agar. The mannitol culture medium used for BC production consisted of 25 g L⁻¹ D-mannitol, 5 g L⁻¹ yeast extract, and 5 g L⁻¹ tryptone.^[1–6] The strain from the agar plate was inoculated into a conical flask containing mannitol culture medium as the seed culture. The initial pH value of the medium was adjusted to 5.0 and was not regulated during the culture. The seed culture was incubated at 30 °C and 130 rpm on a rotary shaker for 2 days, and 6 mL of this seed culture was inoculated into a 100 mL culture medium in 600 mL conical flask for the production of BC. The cultivation was carried out starting at pH 5.0 and 30 °C in a static incubator for 10 days. After incubation, the BC pellicles produced on the surface of the mannitol culture medium were harvested and washed first with a 1% (w/v) aqueous NaOH at 90 °C for 15 min, then with deionized water to remove all microbial product contaminants and obtain purified pellicles.^[1–6]

Preparation of BC Particles and BC-ALG Mixed Slurries: To prepare BC slurries for freeze casting, the BC pellicles were broken down into particles with a cryomill (Retsch, Model 2013, Haan, Germany) using a precooling step at 5 Hz for 20 min and a cryomilling step at 30 Hz for 30 min. The whole procedure was carried out at liquid nitrogen temperature (−196 °C). The resulting BC particles retained BC's unique network structure with nanometer-scale pores. After cryomilling, the BC particles were mixed with the binder sodium alginate solution (4.8 wt%) in a shear mixer (SpeedMixer DAC 150 FVZ-K, FlackTek Inc, Landrum, SC) at 3000 rpm for 2 min, to form homogenous BC-ALG mixed slurries (5.0 wt% BC and 0.9 wt% sodium alginate in the slurries) prior to freeze casting.

Preparation of Freeze-Cast BC Foams by Freeze Casting: To prepare foams, the BC-sodium alginate slurries were freeze-cast with a cooling rate of 10 °C min⁻¹ applied from 2 to −150 °C in a custom-made freeze-casting system. Once the BC-ALG samples were fully frozen, they were removed from the mold with an arbor press and lyophilized in a FreeZone 4.5 L lyophilizer (Labconco, Kansas City, MS) for 3 days to obtain BC foams.

Carbonization of Freeze-Cast BC-ALG Foams: For carbonization, the freeze-cast BC-ALG foams were placed in cylindrical graphite boats of 50.8 mm length, and inner and outer diameters of 25.4 and 38.1 mm, respectively. The graphite boats were closed with a graphite lid, and placed in a vacuum furnace (ABAR 90, ABAR Corporation, Kleve, Germany). After evacuating the furnace chamber to 5–10 mmHg (0.7–1.3 kPa), it was heated at 3 °C min⁻¹ to 400 °C and held at this temperature for 2 h to remove moisture and volatile materials from the samples. While at 400 °C, the furnace chamber was three times purged and back-filled with Argon until the chamber pressure reached 3 psig (20 kPa) to protect the foams and graphite boats from oxidation during the following carbonization process. For carbonization, the foams were heated at a rate of 10 °C min⁻¹ from

400 °C to the respective carbonization temperature of 1000, 1100, or 1200 °C, held at the carbonization temperature for 1 h, and cooled to RT at 10 °C min⁻¹.

Structural Characterization: In order to obtain freeze-cast foams with undisturbed cross sections for structural characterization, the freeze-cast BC-ALG cylinders were first cut parallel and perpendicular to the freezing direction, in the frozen state using a Japanese “Kugihiki” flush cutting hand saw. Samples for imaging were taken from the center of the sample at a height of 17.5 mm measured from the sample bottom. In a second sample preparation step, the saw-cut cross-sections were smoothed with a microtome (Delaware Diamond Knives, Inc. Wilmington, DE) in a -10 °C cold room. Once microtomed, the samples were freeze dried for 3 days in a FreeZone 4.5 L lyophilizer. A few of these freeze-cast BC-ALG foams with smooth cross sections were carbonized as detailed in the section on “Carbonization of Freeze-Cast BC-ALG Foams” above. Both the freeze-cast BC-ALG foams and the carbonized BC-ALG foams were sputtered with a 10 nm thick carbon conductive layer (Hummer 6.2 sputtering system, Anatech Inc., Union City, CA) for observation with a scanning electron microscope (SEM, FEI XL-30 FEG ESEM, Hillsboro, OR) at accelerating voltages of 2 to 5 kV. Mean values and standard deviations for the pore length, width and their aspect ratios were determined on SEM micrographs of cross sections cut perpendicular to the freezing direction using ImageJ (ImageJ, U.S. National Institutes of Health, Bethesda, MD). Before analysis, the scale in ImageJ was calibrated to match the scale bar of the SEM micrographs. About 20–30 pores in SEM micrographs were accurately selected using the “threshold function” in ImageJ carefully adjusting the “threshold color” for measurement. Sets of measurements for pore length and width were obtained using the “straight function” in ImageJ on SEM micrographs of the cross sections cut perpendicular to the freezing direction for the freeze-cast BC-ALG foam and the carbonized freeze-cast BC-ALG foam, respectively.

Electrical Conductivity Characterization: The electrical conductivity, σ , of the carbonized BC-ALG foams was determined with a standard four-point probe (Signatone, Model S-301-4, Gilroy, CA) on 5–6 mm thick layers cut from the carbonized freeze-cast BC-ALG foam scaffolds. The 5 mm thick layers were cut centering them at three standard heights: 5 mm (bottom), 10.5 mm (middle), and 16 mm (top), thus layers extending from 2.5–7.5 mm, 8–13 mm, and 13.5–18.5 mm measured from the sample bottom surface at which freezing had started. Each of the four probes had a tip radius of 254 μm (0.01 in) and a probe center spacing of 1.27 mm (50 mil). To measure the electrical conductivity of the sample, a defined current was passed through the two outer probes and the voltage measure between the inner probes.^[67] Because the sample thickness was greater than half the probe spacing, Equation (6) was used to calculate the electrical conductivity of the material to correct for geometrical effects that resulted from the fact that the samples were neither a bulk nor a sheet sample (thickness is less than half the probe spacing)^[68]

$$\sigma = \frac{I}{U} \frac{\ln\left(\frac{\sinh\left(\frac{t}{s}\right)}{\sinh\left(\frac{t}{2s}\right)}\right)}{\pi t} \quad (6)$$

where t is the thickness, s is the probe spacing (50 mil = 1.27 mm), U is the voltage across the inner probe, I is the current in outer probes, and ρ and σ are resistivity and electrical conductivity, respectively.

Raman Spectroscopy: To determine the degree of carbonization, the Raman spectra for the carbonized freeze-cast BC-ALG foam samples processed at different carbonization temperatures (1000, 1100, and 1200 °C) were obtained with a confocal Raman microscope CRM 200 (WITec GmbH, Ulm, Germany) and a 514.4 nm excitation wavelength laser source. For spectroscopy, the samples were placed on an x-y translation stage with 20 mm \times 20 mm travel and a <1 μm resolution and the wavenumber range for the spectra chosen as 800–2000 cm^{-1} .

To remove fluorescent backgrounds from Raman spectra, the baseline was subtracted from the raw data. In a second step, the intensity of the spectra was normalized for comparison. The D and G peaks of the Raman spectra were fit with Lorentzian curves using Origin (OriginLab Corporation, Northampton, MA). The R^2 values were in the range of 0.992–0.998.

Mechanical Characterization: Compression tests both parallel and perpendicular to the freezing direction were performed to determine the mechanical properties of freeze-cast BC-ALG foams before and after carbonization. For the freeze-cast BC-ALG foams, cubes with 5 mm side length were cut at three standard heights from the samples, measured from the bottom of the sample with cube centers at 7 mm (bottom, 4.5–9.5 mm), 17.5 mm (middle, 15–20 mm), and 28 mm (top, 25.5–30.5 mm) using a Well 4240 wire saw with a wire speed of 0.6 m s^{-1} and a diamond-decorated steel wire diameter of 220 μm . Also for the corresponding carbonized BC-ALG foams, cubes with 5 mm side length were cut at three standard heights from the samples using a Well 4240 wire saw with the same wire speed. However, to take into account the shrinkage during carbonization, the heights were adjusted to cube centers at 4.5 mm (bottom, 2–7 mm), 10 mm (middle, 7.5–12.5 mm), and 15.5 mm (top, 13–18 mm) measured from the sample bottom. After manufacturing and preparation of the samples, they were conditioned and tested at ambient environment in lab, at room temperature (about 22–24 °C) and lab relative humidity (about 52–55%). The compression tests were conducted on an Instron 5948 (Instron, Norwood, MA) with a 5 N load cell. The samples were tested both parallel and perpendicular to the freezing direction at a strain rate of 0.01 s^{-1} , which corresponded to a crosshead speed of 0.05 mm s^{-1} . Young’s modulus, yield strength, and toughness were obtained from compressive stress–strain curves.^[27,28]

Acknowledgements

The authors thank Prof. M. Ackerman of the Thayer School of Engineering, Dartmouth College for allowing the use of the equipment in her lab for the BC cultivation. The authors thank J. Wu from Department of Materials Science, Lawrence Berkeley National Lab for assisting with the carbonization of the samples. The authors thank Dr. C. Daghlian from Dartmouth Electron Microscope Facility for expert SEM and Raman training and experimental assistance. Financial support through DOE Grant DE-AC07-05ID14517 (NEUP10-848), NIH-NICHD Grant R21HD87828, and NSF-CMMI Grant 1200408 are gratefully acknowledged.

Conflict of Interest

The authors declare no conflict of interest.

Data Availability Statement

The data that supports the findings of this study are available in the supplementary material of this article.

Keywords

compression, electrical conductivity, hierarchical porosity, modulus, strength

Received: June 11, 2021
Revised: September 8, 2021
Published online:

- [1] K. Qiu, A. N. Netravali, *Polym. Rev.* **2014**, *54*, 598.
- [2] K. Qiu, A. N. Netravali, in *Recent Advances in Adhesion Science and Technology in Honor of Dr. Kash Mittal*, (Eds: W. Gutowski, H. Dodiuk), CRC Press, Boca Raton, FL **2014**, pp. 193–208.
- [3] K. Qiu, A. N. Netravali, *J. Mater. Sci.* **2012**, *47*, 6066.
- [4] A. N. Netravali, K. Qiu, *US Patent 9499686 B2*, **2013**.
- [5] F. Hong, K. Qiu, *Carbohydr. Polym.* **2008**, *72*, 545.
- [6] K. Qiu, A. N. Netravali, in *Biodegradable Polymers. Advancement in biodegradation study and applications*, Vol. 1 (Ed: C. C. Chu), Nova Science Publishers, Inc., New York, NY **2015**, pp. 325–379.
- [7] K. Qiu, A. Netravali, *Fibers* **2017**, *5*, 31.
- [8] Y. C. Hsieh, H. Yano, M. Nogi, S. J. Eichhorn, *Cellulose* **2008**, *15*, 507.
- [9] H. Backdahl, G. Helenius, A. Bodin, U. Nannmark, B. R. Johansson, B. Risberg, P. Gatenholm, *Biomaterials* **2006**, *27*, 2141.
- [10] M. Iguchi, S. Yamanaka, A. Budhiono, *J. Mater. Sci.* **2000**, *35*, 261.
- [11] D. Klemm, B. Heublein, H. P. Fink, A. Bohn, *Angew. Chem., Int. Ed.* **2005**, *44*, 3358.
- [12] D. Klemm, D. Schumann, U. Udhardt, S. Marsch, *Prog. Polym. Sci.* **2001**, *26*, 1561.
- [13] F. Liebner, N. Aigner, C. Schimper, A. Potthast, T. Rosenau, in *Functional Materials from Renewable Sources*, Vol. 1107 (Eds: F. Liebner, T. Rosenau), American Chemical Society, Washington, DC **2012**, pp. 57–74.
- [14] J. D. Fontana, A. M. Desouza, C. K. Fontana, I. L. Torriani, J. C. Moreschi, B. J. Gallotti, S. J. Desouza, G. P. Narcisco, J. A. Bichara, L. F. X. Farah, *Appl. Biochem. Biotechnol.* **1990**, *24–25*, 253.
- [15] A. Svensson, E. Nicklasson, T. Harrah, B. Panilaitis, D. L. Kaplan, M. Brittberg, P. Gatenholm, *Biomaterials* **2005**, *26*, 419.
- [16] Y. Z. Wan, L. Hong, S. R. Jia, Y. Huang, Y. Zhu, Y. L. Wang, H. J. Jiang, *Compos. Sci. Technol.* **2006**, *66*, 1825.
- [17] J. A. Westland, R. S. Stephens, W. C. Johnston, H. J. Rosenkrans, *US Patent 5207826*, **1993**.
- [18] W. K. Wan, J. L. Hutter, L. Milton, G. Guhados, in *Cellulose Nanocomposites*, Vol. 938 (Eds: K. Oksman, M. Sain), American Chemical Society, Washington, DC **2006**, pp. 221–241.
- [19] H. Shibazaki, S. Kuga, F. Onabe, M. Usuda, *J. Appl. Polym. Sci.* **1993**, *50*, 965.
- [20] U. G. K. Wegst, H. Bai, E. Saiz, A. P. Tomsia, R. O. Ritchie, *Nat. Mater.* **2015**, *14*, 23.
- [21] S. Deville, *Materials* **2010**, *3*, 1913.
- [22] S. Deville, *J. Mater. Res.* **2013**, *28*, 2202.
- [23] B. W. Riblett, N. L. Francis, M. A. Wheatley, U. G. K. Wegst, *Adv. Funct. Mater.* **2012**, *22*, 4920.
- [24] M. M. Porter, J. Mckittrick, M. A. Meyers, *JOM* **2013**, *65*, 720.
- [25] U. G. K. Wegst, M. Schechter, A. E. Donius, P. M. Hunger, *Philos. Trans. R. Soc., A* **2010**, *368*, 2099.
- [26] P. M. Hunger, A. E. Donius, U. G. K. Wegst, *J. Mech. Behav. Biomed. Mater.* **2013**, *19*, 87.
- [27] P. M. Hunger, A. E. Donius, U. G. K. Wegst, *Acta Biomater.* **2013**, *9*, 6338.
- [28] A. E. Donius, A. D. Liu, L. A. Berglund, U. G. K. Wegst, *J. Mech. Behav. Biomed. Mater.* **2014**, *37*, 88.
- [29] Q. Fu, M. N. Rahaman, F. Dogan, B. S. Bal, *Biomed. Mater.* **2008**, *3*, 025005.
- [30] Z. Y. Wu, C. Li, H. W. Liang, J. F. Chen, S. H. Yu, *Angew. Chem., Int. Ed.* **2013**, *52*, 2925.
- [31] L. F. Chen, Z. H. Huang, H. W. Liang, Q. F. Guan, S. H. Yu, *Adv. Mater.* **2013**, *25*, 4746.
- [32] H. Hu, Z. B. Zhao, W. B. Wan, Y. Gogotsi, J. S. Qiu, *Adv. Mater.* **2013**, *25*, 2219.
- [33] X. W. Mao, F. Simeon, G. C. Rutledge, T. A. Hatton, *Adv. Mater.* **2013**, *25*, 1309.
- [34] B. Wang, X. L. Li, B. Luo, J. X. Yang, X. J. Wang, Q. Song, S. Y. Chen, L. J. Zhi, *Small* **2013**, *9*, 2399.
- [35] W. Luo, J. Schardt, C. Bommier, B. Wang, J. Razink, J. Simonsen, X. L. Ji, *J. Mater. Chem. A* **2013**, *1*, 10662.
- [36] L. B. Deng, R. J. Young, I. A. Kinloch, Y. Q. Zhu, S. J. Eichhorn, *Carbon* **2013**, *58*, 66.
- [37] H. W. Liang, Q. F. Guan, L. T. S. Zhu-Zhu, H. B. Yao, X. Lei, S. H. Yu, *NPG Asia Mater.* **2012**, *4*, e19.
- [38] X. W. Lu, P. J. Pellechia, J. R. V. Flora, N. D. Berge, *Bioresour. Technol.* **2013**, *138*, 180.
- [39] C. Walter, S. Barg, N. Ni, R. C. Maher, E. Garcia-Tunon, M. M. Z. Ismail, F. Babot, E. Saiz, *J. Eur. Ceram. Soc.* **2013**, *33*, 2365.
- [40] H. Vafaenezhad, S. M. Zebarjad, J. V. Khaki, *Adv. Mater. Res.* **2012**, *413*, 95.
- [41] M. F. Ashby, *Philos. Trans. R. Soc., A* **2006**, *364*, 15.
- [42] A. K. Kercher, D. C. Nagle, *Carbon* **2002**, *40*, 1321.
- [43] Y. R. Rhim, D. J. Zhang, D. H. Fairbrother, K. A. Wepasnick, K. J. Livi, R. J. Bodnar, D. C. Nagle, *Carbon* **2010**, *48*, 1012.
- [44] M. K. van der Lee, A. J. van Dillen, J. W. Geus, K. P. de Jong, J. H. Bitter, *Carbon* **2006**, *44*, 629.
- [45] A. Mizoguchi, J. Shioya, Y. Yamaguchi, Y. Ueba, *US Patent 4919779*, **1990**.
- [46] A. Mizoguchi, J. Shioya, Y. Yamaguchi, Y. Ueba, H. Matsubara, *US Patent 4795656*, **1989**.
- [47] V. Chabot, B. Kim, B. Sloper, C. Tzoganakis, A. Yu, *Sci. Rep.* **2013**, *3*, 1378.
- [48] S.-J. Park, *Carbon Fibers*, Springer, Dordrecht **2015**.
- [49] A. Lekawa-Raus, J. Patmore, L. Kurzepa, J. Bulmer, K. Koziol, *Adv. Funct. Mater.* **2014**, *24*, 3661.
- [50] Y. Pauleau, P. B. Barna, *Protective Coatings and Thin Films: Synthesis, Characterization and Applications*, Springer, Dordrecht **1996**.
- [51] H. O. Pierson, *Handbook of Carbon, Graphite, Diamond and Fullerenes: Properties, Processing and Applications*, Noyes Publications, Park Ridge, NJ **1993**.
- [52] B. Dai, Y. Ren, G. H. Wang, Y. J. Ma, P. Zhu, S. R. Li, *Nanoscale Res. Lett.* **2013**, *8*.
- [53] Y. Li, H. Zhu, F. Shen, J. Wan, X. Han, J. Dai, H. Dai, L. Hu, *Adv. Funct. Mater.* **2014**, *24*, 7366.
- [54] H.-C. Hwang, J. S. Woo, S.-Y. Park, *Carbohydr. Polym.* **2018**, *196*, 168.
- [55] L. J. Gibson, *J. Biomech.* **2005**, *38*, 377.
- [56] L. J. Gibson, M. F. Ashby, B. A. Harley, *Cellular Materials in Nature and Medicine*, Cambridge University Press, Cambridge **2010**.
- [57] L. J. Gibson, M. F. Ashby, *Cellular Solids: Structure and Properties*, Cambridge University Press, Cambridge **1999**.
- [58] M. Ul-Islam, J. H. Ha, T. Khan, J. K. Park, *Carbohydr. Polym.* **2013**, *92*, 360.
- [59] E. Tsouko, C. Kourmentza, D. Ladakis, N. Kopsahelis, I. Mandala, S. Papanikolaou, F. Paloukis, V. Alves, A. Koutinas, *Int. J. Mol. Sci.* **2015**, *16*, 14832.
- [60] AZOMaterials, AZO Materials **2001**, <https://www.azom.com/properties.aspx?ArticleID=516> (accessed: May 2021).
- [61] F. Lai, Y.-E. Miao, L. Zuo, Y. Zhang, T. Liu, *ChemNanoMat* **2016**, *2*, 212.
- [62] C. Antonini, T. Wu, T. Zimmermann, A. Kherbeche, M.-J. Thoraval, G. Nyström, T. Geiger, *Nanomaterials* **2019**, *9*, 1142.
- [63] X. Wang, D. Kong, B. Wang, Y. Song, L. Zhi, *Sci. China: Chem.* **2016**, *59*, 713.
- [64] R. Liu, L. Ma, S. Huang, J. Mei, J. Xu, G. Yuan, *New J. Chem.* **2017**, *41*, 857.
- [65] S. Bouissil, Z. El Alaoui-Talibi, G. Pierre, P. Michaud, C. El Modafar, C. Delattre, *Molecules* **2020**, *25*, 720.
- [66] A. Boucelkha, E. Petit, R. Elbouchafait, R. Molinié, S. Amari, R. Z. Yahaoui, *J. Appl. Physcol.* **2017**, *29*, 509.
- [67] F. M. Smits, *Bell Syst. Tech. J.* **1958**, *37*, 711.
- [68] D. K. Schroder, *Semiconductor Material and Device Characterization*, Wiley, Hoboken, NJ **2006**.